



Assessment of the RegCM4 Performance in Simulating the Surface Radiation Budget and Hydrologic Balance Variables in South America

David Pareja-Quispe¹ · Sergio Henrique Franchito¹ · Julio Pablo Reyes Fernandez^{1,2}

Received: 19 May 2021 / Revised: 16 July 2021 / Accepted: 3 August 2021 / Published online: 14 August 2021
© The Author(s) 2021

Abstract

The ability of the Regional Climate Model v4 (RegCM4) to simulate the surface radiation budget and hydrological balance variables over South America have been evaluated. For this purpose, a 34-year long simulation was carried out with the regional climate model RegCM4 over South America on the CORDEX domain. The model is forcing by ERA-Interim reanalysis. The results show that RegCM4 simulates the main patterns of the variables associated with the surface radiation budget and hydrological balance in the four seasons of the year compared to the observations (CLARA2 and CRU/PERSIANN). However, the cloudiness and surface radiation budget variables: Cloud Fraction Cover (CFC), net shortwave (SW) and longwave (LW) radiation at surface are overestimated, mainly over the oceans. This is associated with the errors in the CFC due to the deficiency of the model in representing the low-level clouds. Some differences are also noted in the hydrological balance. The intensity and temporal evolution of precipitation, especially in the central and southern Amazon, may be associated with the selected domain, which fails to adequately represent the influence of the adjoining oceans. In northern and northeast parts, the differences are associated with deficiencies of RegCM4 in representing precipitation rates. Although the deficiencies, taking into account that the model is capable to reproduce the general pattern of some important variables of the surface radiation budget and hydrological cycle, it may be a useful tool for climate studies.

Keywords RegCM4 · South America · Surface radiation budget · Hidrologic cycle

1 Introduction

The surface radiative balance and hydrologic cycle are responsible for various atmospheric processes such as precipitation, evapotranspiration, wind intensity and temperature, in the regional and global scales (Wallace and Hobbs 2006). They are particularly important in tropical regions since the amount of radiation and the rates of precipitation are higher. South America (SA) region (between the latitudes 56° S–12° N) is influenced by several processes that occur in the middle and tropical latitudes, as well as their interactions. SA is strongly affected by the adjoining oceans (Pacific and Atlantic) where the sea surface temperature (SST) variability controls the seasonal migration and

interannual variation of the Intertropical Convergence Zone (ITCZ) and South Atlantic Convergence Zone (SACZ) (Garreaud et al. 2009; Reboita et al. 2010). These large-scale characteristics strongly affect the SA tropical and subtropical precipitation regimes. Also, the complex topography of the Andes mountains along the west of the continent, the vegetation of the Amazon basin and the large amount of radiation received by the tropical region maintain the SA weather and climate characteristics (Garreaud et al. 2009; Nobre et al. 2009; Reboita et al. 2010).

Some variables of the hydrological cycle is directly linked to the changes in the radiation balance and atmospheric temperature (Inglezakis et al. 2016). The northern part of SA, where the Amazon basin is located, is characterized by the large quantity of solar radiation received. The solar radiation received at the top of the atmosphere between 5° N and 10° S varies from the maximum of 424.8 Wm⁻² in December-January to the minimum of 355.3 Wm⁻² in June-July (Salati and Marques 1984). At the surface, the incident solar radiation is around 185.2–208.3 Wm⁻² (Pereira et al. 2017). The seasonal cycle of incident solar radiation in the central

✉ David Pareja-Quispe
davidp157@gmail.com

¹ National Institute for Space Research, São José dos Campos, SP, Brazil

² Center for Weather Forecast and Climatic Studies, Cachoeira Paulista, SP, Brazil

Amazon shows maximum values in September–October and minimum values in December–February (Culf et al. 1996; Pereira et al. 2017). This temporal distribution is in the major part controlled by the nebulosity associated with Amazon convection (Horel et al. 1989).

The net surface shortwave (SW) and longwave radiation (LW) budget are important in climate modeling because they regulate the energy balance of the Earth and control the diurnal and annual cycles (Kothe et al. 2011). In the context of the CLARIS-LPB Project (Europe-South America Network for Climate Change Assessment and Impact Studies in La Plata Basin), Pessacg et al. (2014) evaluated the net surface shortwave and longwave radiation in the SA using seven regional models with a spatial resolution of around 50 km for the period from 1990 to 2008. Their results showed that in the most of the regional models the net SW is overestimated in the tropical regions of SA and La Plata basin, and underestimated over the ocean during the austral summer and winter seasons. The net LW did not show a defined pattern in the analyzed models, each one of them showing different results. On the other hand, the evaluations done by Lange et al. (2015) and Brisson et al. (2016) showed that parameterization of the convection and subgrid-scale clouds can improve the deficient representation of cloud cover, precipitation, and surface radiation budget, thus reducing biases. In the hydrological cycle, the precipitation is the meteorological variable more analyzed because it is the result of several physical processes including the thermodynamic, the changes in the water phase, and net radiation among others. In the Amazon, in the rainiest region of SA, the precipitation rates are maintained by the evapotranspiration, which is recycled by local sources (Salati et al. 1979; Zemp et al. 2017), the moisture carried from the Atlantic tropical ocean by the trade winds (Drumond et al. 2008; Duran-Quesada et al. 2009; Zemp et al. 2017) and the water vapor flux convergence associated to the regional and large-scale circulations (Chen 1985; Nobre et al. 2009). On the other hand, evapotranspiration is a dominant way in which the arriving net radiation and the precipitation are transferred from the surface to the atmosphere (Nepstad et al. 2004; da Rocha et al. 2009). On the regional scale, the moisture transport inside and outside from Amazon is extremely important for the rainfall regime, particularly during the rainy season. The moisture exported outside from Amazon is transported to the east of the Andes mountains by the SA Low-Level Jets (LLJs), with a maximum wind speed of 15 ms^{-1} at 850 hPa, near 17° S and 62° W . This contributes to the precipitation in the La Plata basin and southeast Brazil (Marengo 2004, 2006; Arraut and Satyamurty 2009; Martinez and Dominguez 2014; Montini et al. 2019).

Although Regional Climate Models (RCMs) are good tools for studying and evaluating the various processes that occur in the different components of the climate system, they still have

some deficiencies in simulating the surface radiation balance and hydrological cycle processes in SA (Pessacg et al. 2014; Chou et al. 2012, 2014; Reboita et al. 2014; Franchito et al. 2014; Lange et al. 2015; Llopart et al. 2017, 2020; Erfanian and Wang 2018). In other regions of the world RegCM4 also shows some deficiencies to represent the atmospheric variables (Giorgi et al. 2012; Chiacchio et al. 2015; Almazroui et al. 2016; Nogherotto et al. 2016). Some studies showed that over Europe the RegCM overestimates the surface net SW radiation by 5 and 60 Wm^{-2} , respectively, in the boreal winter (December–January and February) and summer (June, July and August), while in the north Africa it is underestimated by -30 to -40 Wm^{-2} . On the other hand, the net LW radiation is underestimated by -40 and -30 Wm^{-2} , respectively, in most part of the model domain and with values 0 Wm^{-2} in the north Africa (Chiacchio et al. 2015). In a similar study, over the north Africa, Panitz et al. (2014) found that the COSMO model underestimates the net SW radiation until -150 Wm^{-2} over the oceanic regions, in January–March and July–September. Over the continent, the values are underestimated by around -50 Wm^{-2} . In the areas where the net SW flux was overestimated the values are around 30 Wm^{-2} . Otherwise, the net LW flux showed underestimated values by around -30 and -40 Wm^{-2} , and overestimated values with the same range of variation.

Particularly, for SA, there are few studies that have been conducted using regional models devoted to the concomitant validation of the surface radiation processes and hydrological cycle. For that purpose, the objective of the present work is to make a simultaneous analysis of these processes using the Regional Climate Model RegCM4 integrated over the Coordinated Regional Climate Downscaling Experiment (CORDEX) domain (Giorgi et al. 2009; Giorgi and Gutowski 2015). This study aims to contribute to a better knowledge of the processes associated with the surface radiation budget and hydrological cycle, especially the precipitation, over SA. Section 2 shows the RegCM4 description, the initial and boundary conditions for the model integration and the observed data used to examine the model performance in simulating the surface radiation balance and hydrological cycle over SA; Sect. 3 contains the results, and the discussions and conclusions are presented in Sects. 4 and 5, respectively. This paper becomes different from earlier studies since the role of the surface SW and LW radiation in the precipitation and potential evapotranspiration is emphasized.

2 Data and Methodology

2.1 Data

Data from the European Centre for Medium-Range Weather Forecasts (ECMWF) ERA-Interim Reanalysis (EIN15) are

used as the initial and boundary conditions in the numerical experiment. This reanalysis is available from January 1979 to August 2019 and has $1.5^\circ \times 1.5^\circ$ (latitude, longitude) spatial resolution, 6 h temporal frequency and 37 vertical levels (Dee et al. 2011). An inter-comparison on reanalysis data made by de Almeida et al. (2018), indicated that in South America the EIN15 shows a better performance in relation to the NCEP-DOE Reanalysis 2 and Climate Forecast System Reanalysis (CFSR) version 1.

The hydrological cycle variables and the water balance (precipitation and potential evapotranspiration) are evaluated using the Climate Research Unit data (CRU, version 4.05), which have a spatial resolution of $0.5^\circ \times 0.5^\circ$ (latitude, longitude) and monthly temporal frequency (Harris et al. 2014, 2020). This dataset is available from 1901 up to the present time. Over the oceans, precipitation data from the Precipitation Estimation from Remotely Sensed Information using Artificial Neural Networks–Climate Data Record (PERSIANN-CDR, hereafter called as PERSIANN) developed by the Center for Hydrometeorology and Remote Sensing (CHRS) of University of California, Irvine (UCI) are used. This data set comprises the globe between the latitudes 60°S – 60°N , with $0.25^\circ \times 0.25^\circ$ (latitude \times longitude) spatial resolution and is available from January 1983 up to the present time (Ashouri et al. 2015). To have the same spatial resolution the PERSIANN data was interpolated to 50 km using a bilinear method.

The radiation balance is evaluated using data from the Climate Monitoring Satellite Application Facility (CM-SAF), Cloud, Albedo, Radiation dataset, AVHRR-based, Edition 2 (CLARA2), derived from the AVHRR (Advanced Very High-Resolution Radiometer), measures the National Oceanic and Atmospheric Administration (NOAA) satellites and Meteorological Operational satellite program (Metop) in polar orbit, as performed by the European Organization for Meteorological Satellites Exploration (EUMETSAT) (Karlsson et al. 2017). The second version is an improvement of the first version, where original visible radiation is intercalibrated and homogenized using the Moderate Resolution Imaging Spectroradiometer (MODIS) data taken as a reference before the application of several parameters' retrievals. The data covers a 34-year period (1982–2015) in the daily and monthly scales and have a $0.25^\circ \times 0.25^\circ$ (latitude, longitude) spatial resolution (Karlsson et al. 2017). The variables used for the analysis are CFC, albedo a net SW and LW radiation. It is available https://doi.org/10.5676/EUM_SAF_CM/CLARA_AVHRR/V002.

The equations for calculating the net SW and LW radiation are:

$$\text{SW} = \text{SIS} (1 - \text{SAL}),$$

$$\text{LW} = \text{SDL} - \text{SOL},$$

where:

SIS = incoming solar surface radiation, SAL = surface Albedo, SDL = surface downwelling longwave radiation, SOL = surface outgoing longwave radiation. Additionally, temperature at 2 m from the CRU dataset is used.

2.2 Methodology

The Regional Climate Model used in the present study is the RegCM4 version 4.5.10 from the International Centre for Theoretical Physics (ICTP) (Giorgi et al. 2012). The model dynamics is based on the Fifth Generation Mesoscale Model (MM5) of the National Center for Atmospheric Research (NCAR)-Pennsylvania State University (PSU) (Grell et al. 1994). RegCM4 is a limited area model for a compressible atmosphere, with Arakawa B-grid and sigma vertical coordinate. It can be used in any region of the world in a wide range of studies (study of processes, climate projections and even paleoclimate). Since its first version in 1989, the RegCM has gone through several updates with the implementation of new schemes of convection, surface, microphysics, etc. (Giorgi et al. 2012). RegCM4 has two surface schemes. In the present study the Biosphere–Atmosphere Transfer Scheme (BATS) is used. Based on Reboita et al. (2014), in the present study the configuration of BATS with MIXED1 convection [Grell (1993) over land and Emanuel and Zivkovic-Rothman (1999) over ocean] is used. In the Conclusions of that paper, the authors recommended the use of this configuration of RegCM4.3 to carry out numerical experiments in the CORDEX domain over SA.

The RegCM4 is continuously running for a 34-year period (1979–2012) using EIN15 data in the CORDEX domain over SA, with the three first years as spin-up. To improve the model simulations, some parameters associated with vegetation type 6 (Amazon forest) in the BATS scheme are modified according to da Rocha et al. (2012) to obtain a better representation of the Amazon soil moisture. These modifications allow us to improve the evapotranspiration rates due to the greater availability of water in the soil column, as described in da Rocha et al. (2012). The modified values are given in Table 1.

The configuration of the RegCM4 used in this study is given in Table 2. Figure 1 shows the model domain of RegCM4, with a spatial resolution of 50 km. To obtain consistency of the analysis, the period of both observations and simulations is the same. So, in this work, the precipitation, potential evapotranspiration, CFC, albedo, temperature at 2 m and net surface LW radiation are analyzed from the period 1982–2012 [31 years (1979–1981 is the spin-up)]. While, the net surface SW radiation is considered from the period 1992–2012 (21 years), both for CLARA2 data and

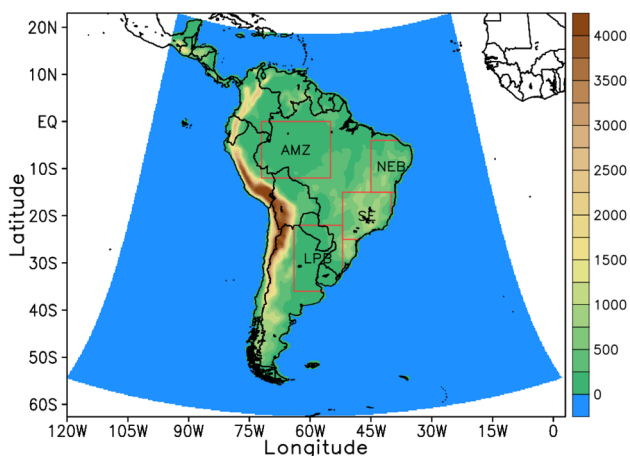
Table 1 Changes to the default configuration of RegCM4 made in this study

Parameters	BATS scheme	
	Default	Modified ^a
deptv (m)	3.0	4.5
deptrv (m)	1.5	3.0
rootf	0.8	0.4
xkxm2 (mm s ⁻¹)	4 × 10 ⁻⁴	1.6 × 10 ⁻⁴

^aFor more details of the parameters modify see da Rocha et al. (2012)

Table 2 Configuration used in the model RegCM4

Model aspects	Options used
Vertical coordinate	σ
Grid horizontal	B-Arakawa
Dynamics	Hydrostatic
Physics	
Radiative transfer	Modified CCM3 (Kiehl et al. 1996)
Planet boundary layer	Modified Holtstag (Holtstag et al. 1990)
Cumulus convection	Grell (continent) (Grell 1993) Emanuel (ocean) (Emanuel and Zivkovic-Rothman 1999)
Microphysic	SUBEX (Pal et al. 2000)
Land surface	BATS (Dickinson et al. 1993)
Ocean fluxes	Zeng (Zeng et al. 1998)
Lateral boundary conditions	Relaxation exponential

**Fig. 1** Model domain, topography (in meters) and region of analysis: Amazon (AMZ), Northeast Brazil (NEB), Southeast Brazil (SE) and La Plata Basin (LPB)

RegCM4 simulation. This is because of the lack of surface incoming SW radiation (the net surface SW radiation is calculated directly from the surface incoming SW radiation and albedo) in most part of tropical and subtropical regions

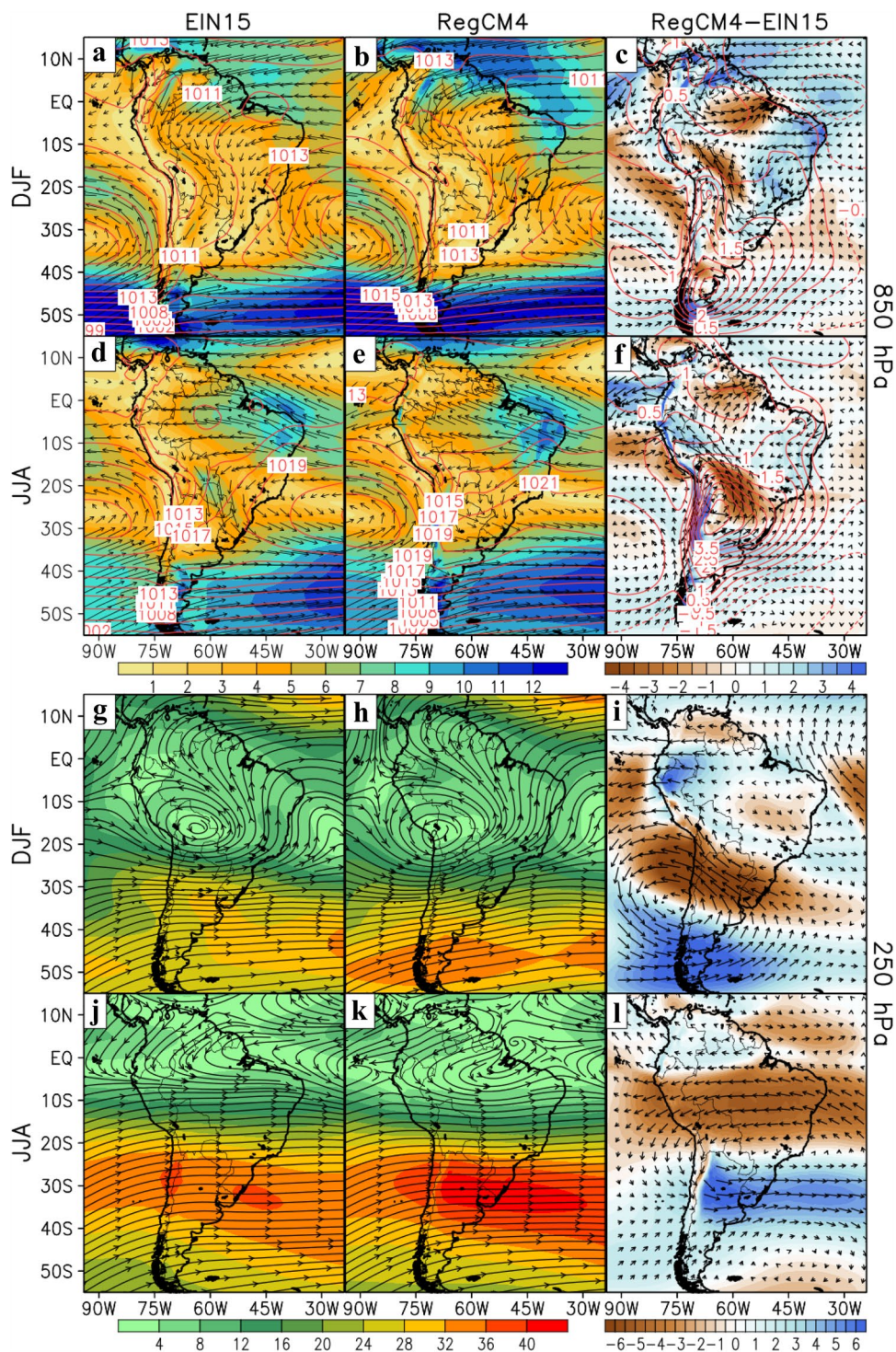
during the period 1982–1991. The potential evapotranspiration calculation in RegCM4 is based on modified version of Penman–Monteith method, which is used in the preparation of CRU data (Harris et al. 2014).

3 Results

3.1 Large-Scale Circulation

Figure 2 shows the comparison between seasonal variation of the horizontal winds simulated by the RegCM4 and the EIN15 at low (850 hPa, Fig. 2a–f) and high levels (200 hPa, Fig. 2g–l). In the austral summer (DJF), at low levels, near Equator, the RegCM4 simulates very well the easterlies trade winds over the Atlantic ocean. The trade winds are responsible for the advection and transport of water vapor from the Atlantic Ocean to the SA continent (Garreaud et al. 2009; Duran-Quesada et al. 2009; Zemp et al. 2017; Zanin and Satyamurty 2020). The Andes cordillera, located in the west SA, acts as an obstacle to the displacement of trade winds so that there is a shift southward along the east region of the mountains (Montini et al. 2019; Zanin and Satyamurty 2020). In the regions of LLJ and northwest Amazon the simulated values are underestimated up to -4 ms^{-1} . In the northeast and north SA the RegCM4 overestimates the wind values up to 4 ms^{-1} . In the austral winter (JJA), the areas where the winds are underestimated and overestimated are the same as in the austral summer, but with low values. The northward and southward displacement of the Pacific and south Atlantic subtropical high is well reproduced by the RegCM4. There is a good agreement between the location of these subtropical highs simulated by the model and their climatological position (Sun et al. 2017; Fahad et al. 2021). At high levels, in the austral summer, the RegCM4 is capable for simulating the main synoptic systems, such as the Bolivian high and the associated cyclonic vortex, as well as the westerlies (Fig. 2h). The RegCM4 shifts westward the Bolivian high compared to that observed in EIN15 (Fig. 2g). Similar deficiencies in the Bolivian high location were found by Llopart et al. (2019). This deficiencies in the simulation of the Bolivian high provoke an anticyclonic circulation in the southwest side of Bolivia, with underestimated values of winds in the north of the circulation and overestimated values in the south of the circulation (Fig. 2i). Erfanian and Wang (2018) also showed that the deficiencies in the representation of the Bolivian high location causes an anticyclonic circulation at high levels in south Bolivia in December. In the austral winter, the westerlies are well simulated by the model. The position of strong westerlies (35° S – 25° S) is well reproduced by the model. However, in the continental region of SA the winds are overestimated up to 6 ms^{-1} , while in oceanic regions the overestimated

Fig. 2 Large-scale circulations climatology (1982–2012) for ERA-Interim (left column), RegCM4 (middle column) and difference between them (right column) for low levels 850 hPa (a–f) and high levels 200 hPa (g–l) for the austral summer (DJF) and winter (JJA). The red lines at the low levels represent the sea level pressure. The unit of wind is ms^{-1}



values are less intense. In contrast, between the 20°S – 5°S , the underestimated values of winds are -5 ms^{-1} . In the other regions of SA the underestimated and overestimated values of winds varies from -2 and 2 ms^{-1} .

In general, the wind pattern simulated by the RegCM4 is similar to that obtained in earlier studies (Fernandez et al. 2006; Seth et al. 2007; Lange et al. 2015; Reboita

et al. 2018a), although the RegCM4 presents higher or lower performance in some regions.

3.2 Surface Radiation Balance

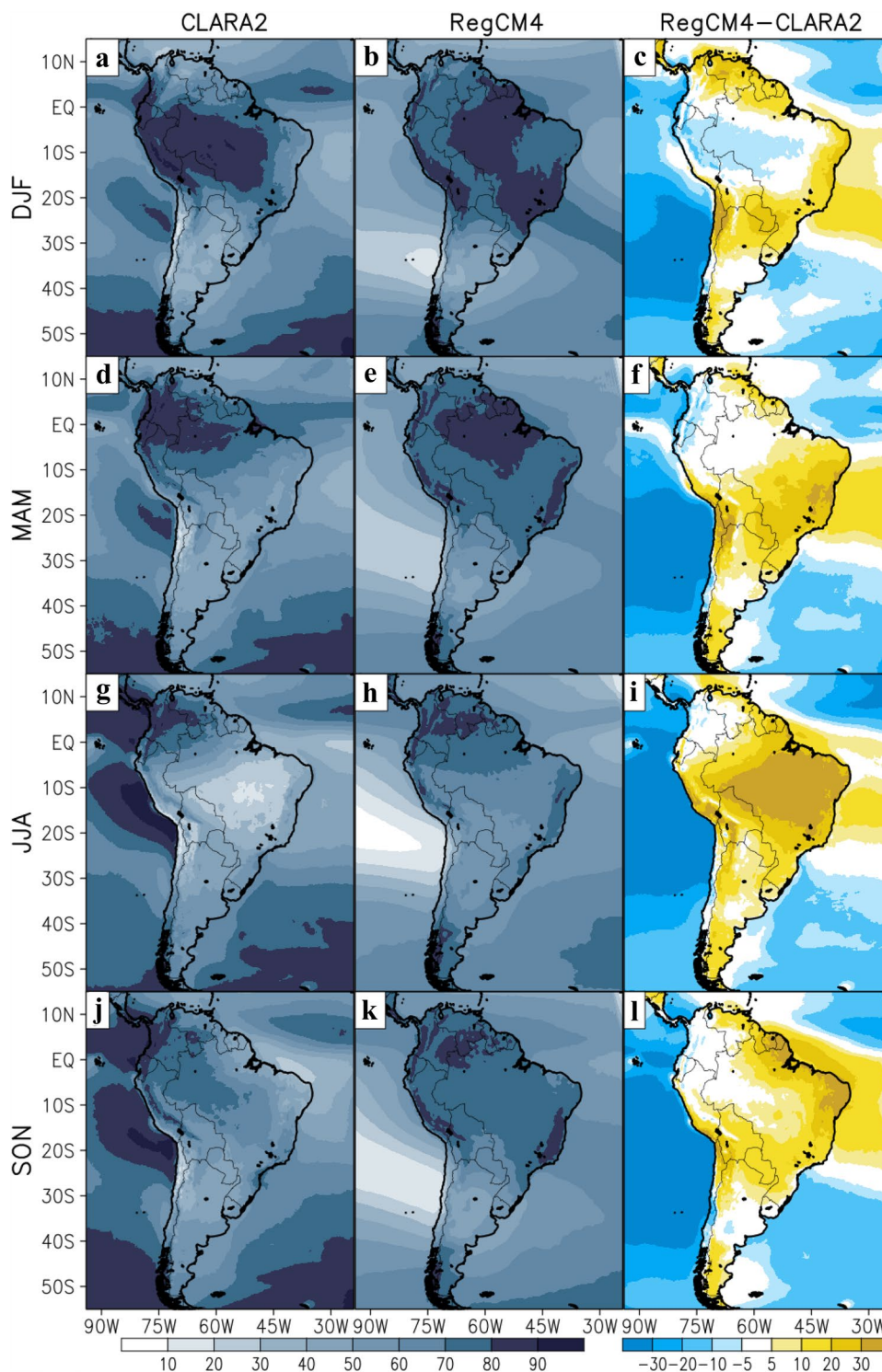
Figure 3 shows, respectively, the seasonal mean (1982–2012) of CFC for the CLARA2 data, RegCM4 simulation and the

difference between them. In the austral summer, which is the rainy season, a higher concentration of CFC is noted in the regions of the ITCZ and the SACZ (Fig. 3a, b). In general, there is a good agreement between the RegCM4 simulation and the distribution of cloud cover observed in CLARA2, mainly over the continent, although over the oceans the agreement is lower (Fig. 3c). In the central SA and parts

of northeast Brazil, the RegCM4 underestimates the cloud cover (around -20%), while in the regions near the eastern littoral of Brazil, parts of central Andes mountains, south and southeast Brazil and Paraguay, the cloud cover is over-estimated (values around $+20\%$).

Over the oceans, the RegCM4 underestimates the CFC with values up to -30% over the north Atlantic ocean and

Fig. 3 Seasonal climatology (1982–2012) of cloud cover fraction (in percent) over South America in CLARA2 (left column), RegCM4 (middle column) and the difference between RegCM4 and CLARA2 (right column)



the Pacific ocean (near Peru and Chile). Simulation for the austral summer is better than the results presented in Lange et al. (2015) because the simulated values are lower (underestimated/overestimated), mainly in the continental region. In the austral autumn, the ITCZ is shifting northwards. From Fig. 3d, e, the region of higher CFC is located toward the north of around 15° S, although the RegCM4 values are underestimated in western Brazil and northwestern SA (values up to -20% in some parts) and overestimated in the eastern and southern part of Brazil (values around +20%) (Fig. 3f). Over the oceans, the spatial distribution of the CFC is similar to that noted in the austral summer. However, the RegCM4 simulation is underestimated (values lower than -30% over the Pacific ocean and up to -20% in the Atlantic ocean).

In the austral winter, the areas with higher CFC are located northward from 3° N (Fig. 3g, h) due to the northward shifting of the ITCZ as a response to the increase of the SST. In the continent, the higher CFC are seen northward from 5° S. Southward from 25° S the CFC is maintained mainly by the frontal systems that occur with more frequency in this season (Andrade and Cavalcanti 2004; Cardozo et al. 2015). The RegCM4 underestimates the CFC in the ITCZ regions (values lower and up to -30% over the Pacific and Atlantic oceans, respectively). On the other hand, in most part of the Andes mountains region, central and east the RegCM4 simulation overestimates the CFC by +5 to +20% (Fig. 3i). For the austral winter, the results of Lange et al. (2015) are better than those of the RegCM4. This may be due to the types of RCMs and the periods of analysis used in these studies. In the austral spring, the ITCZ starts moving southwards so that the CFC configuration is similar to that observed in the austral summer, mainly over the continent (Fig. 3j). There is a good agreement between the RegCM4 simulation and the CLARA2 data, as seen in Fig. 3j, k. However, the RegCM4 values are underestimated in the central and northwest SA and parts of Argentina and Paraguay (around -5 to -20%), while in some parts of the northeast and south of SA, they are overestimated by +5% to +20% (Fig. 3l). Again, the CFC is underestimated by the RegCM4 over the oceans.

Figure 4 shows the mean seasonal net SW at surface for the CLARA2 data, RegCM4 simulations and the difference between them, for the period 1992–2012. As can be seen in Fig. 4a–c, the RegCM4 is able to reproduce the spatial distribution of SW in the austral summer. As noted in Fig. 4c, northward from 20° S over the continent, the SW fluxes are lower compared to the rest of the continent because the simulated CFC (and precipitation) are higher in this season. Otherwise, over the oceans the simulated SW fluxes are overestimated in the regions where the CFC is underestimated. The areas where the simulated values are overestimated agree with the spatial pattern of the observed CFC. In

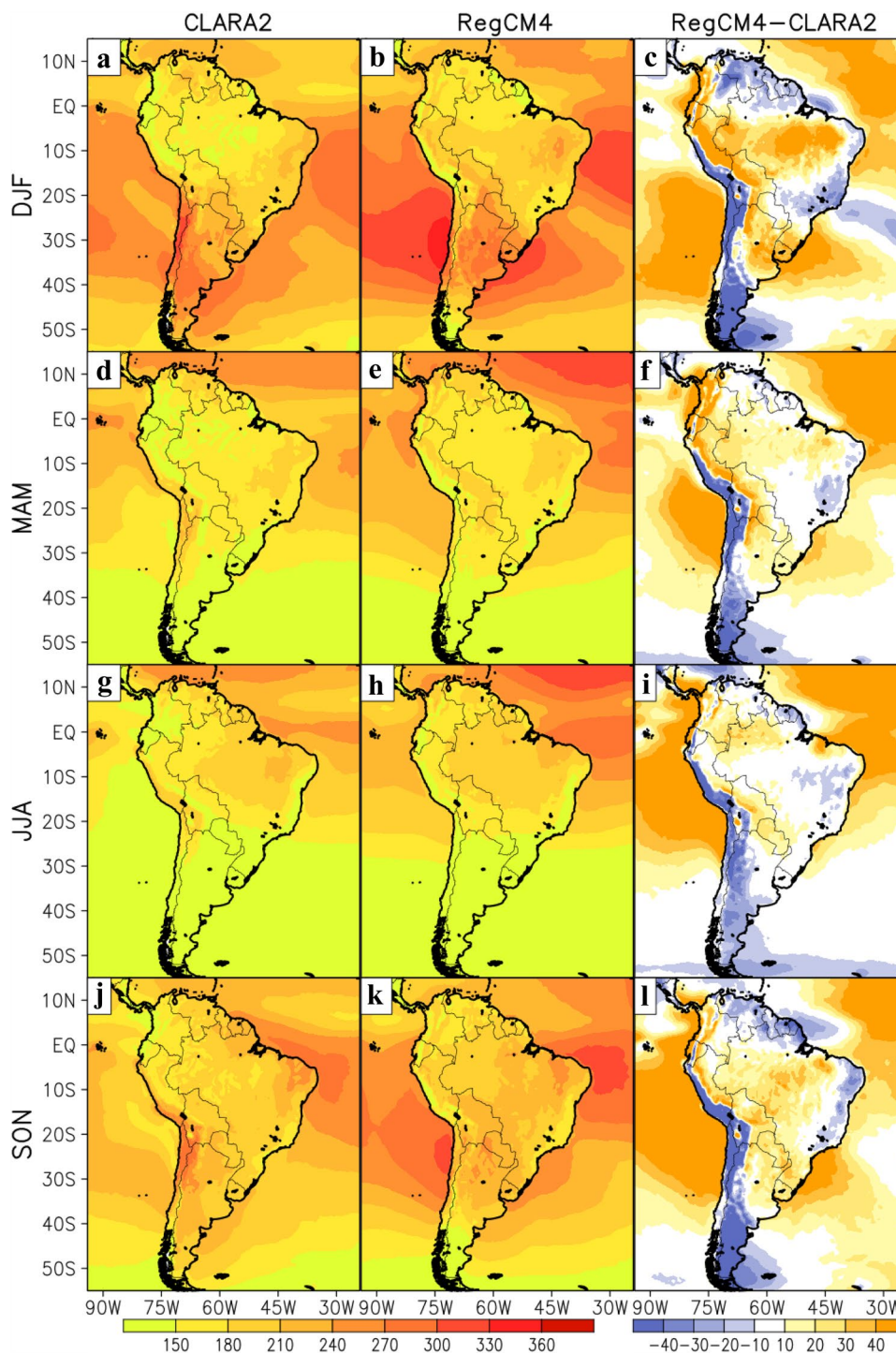
some parts of the Pacific ocean, mainly in the regions near the littoral of Peru and Chile as well as some regions of the Atlantic ocean, the overestimated values show areas where SW are higher than +40 Wm⁻². This may be due to the fact that the RegCM4 is not able to simulate adequately the low-level cloud cover which is dominant in the regions. Garreaud et al. (2007) showed that in the coastal regions of Peru and Chile this kind of cloud is due to the thermal inversion which occurs between 1 and 2 km height.

In addition, in these regions there is wind subsidence caused by the South Pacific Subtropical High (SPSH). As showed in Fig. 7.6 of Boucher et al. (2013), the low-level clouds are mainly located in the oceanic regions. In the austral autumn and spring, the surface net SW in the continent is underestimated in the entire region of Andes mountain, while in central SA it is overestimated (Fig. 4f, i), with values close to those observed in the austral summer (Fig. 4c). In the austral winter, the RegCM4 simulation of SW is better than in the other seasons. In most of the continent, the values of SW are slightly overestimated (Fig. 4g–i). In the Andes region, the simulated values are underestimated by around -30 Wm⁻². Similar to the other seasons, in some parts of the ocean regions, the simulated SW values are overestimated due to the fact that the model is not able to simulate adequately the low-level clouds.

Figure 5 shows the seasonal spatial distribution of the net LW at the surface (CLARA2, RegCM4 simulations and the difference between them). It can be noted, in all the seasons the RegCM4 simulations of the net LW shows lower differences compared to that observed in CLARA2 data than in the case of the simulations of the net SW (Fig. 4). In the austral summer (Fig. 5a–c), the net LW is underestimated by the RegCM4 in the central SA (around -10 to -20 Wm⁻²), while southward of 20° S, over the Andes mountains, the underestimated values are up to -40 Wm⁻². Regions of underestimated values of the net LW up to -40 Wm⁻² are also seen in the eastern Pacific near the littoral of Peru and Chile. Otherwise, over some regions of the Atlantic Ocean, the net LW is overestimated, but with smaller values compared to the underestimated regions. In the austral autumn and spring, the spatial distribution of the positive and negative biases in the continent (Fig. 5f, l) is similar to that obtained in the austral summer (Fig. 5c), although the values of the biases are lower. These results are better than previous version of RegCM4 (Pessacg et al. 2014), especially in the summer and winter seasons.

Over the oceans, the spatial distribution of the positive biases in the austral autumn is similar to that noted in the austral summer, while in the austral spring the spatial pattern of the biases and the austral winter are alike (Fig. 5i). As can be seen in Fig. 5g–i, in this season, the RegCM4 shows better performance in reproducing the observed LW. However, the observed values of LW are higher (Fig. 5g)

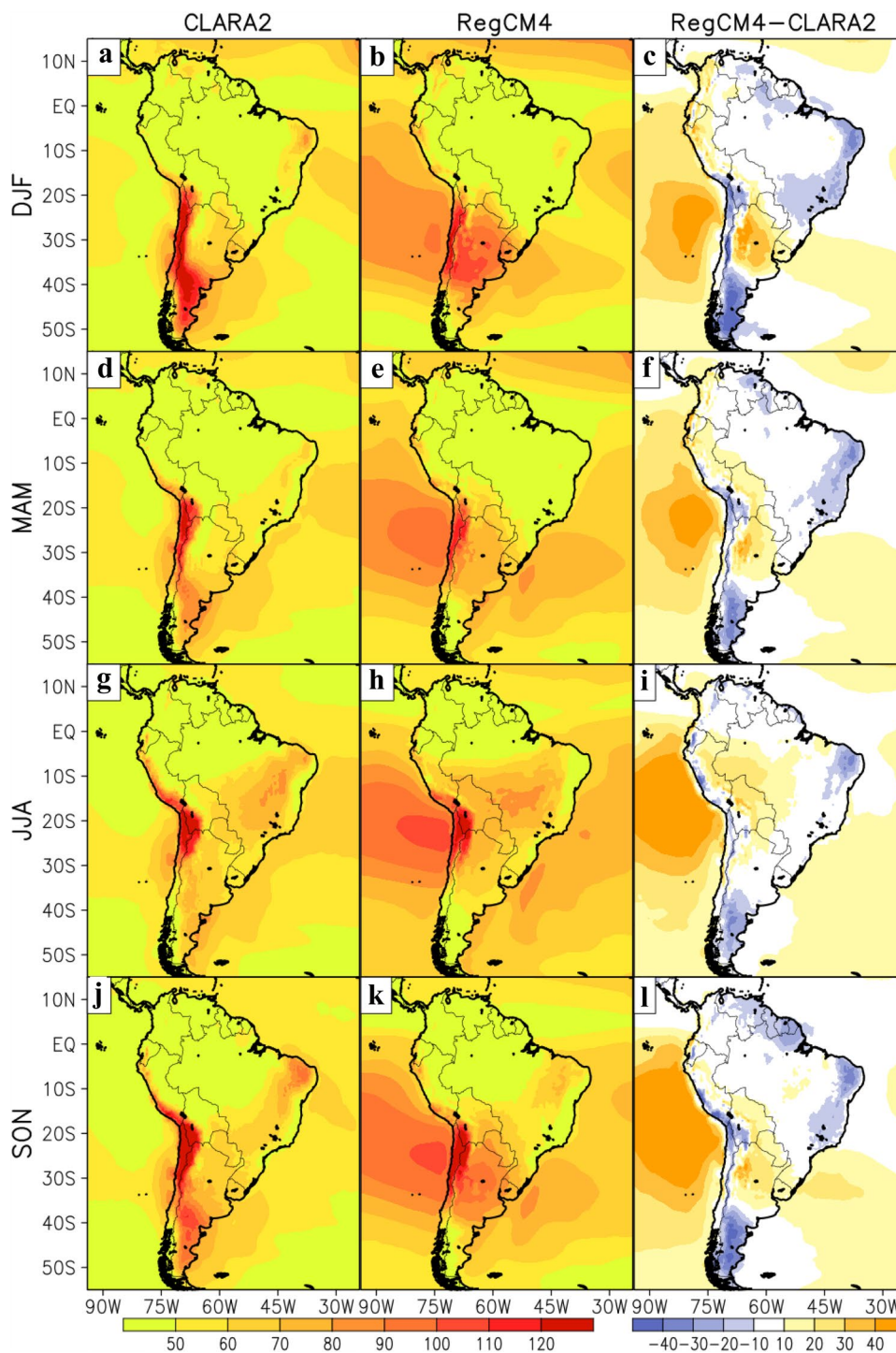
Fig. 4 As in Fig. 3, but for the net shortwave radiation at surface (Wm^{-2}) for 1992–2012 period



due to the lower CFC (Fig. 3a) during the dry season. In the center-west of SA the simulated values of LW are overestimated, with some areas showing values up to $+20 \text{ Wm}^{-2}$. In the Andes region, the simulated values are underestimated (around -10 Wm^{-2}). In the Pacific ocean, near the littoral of Chile and Peru, the region of overestimated values reaches $+40 \text{ Wm}^{-2}$, while in the Atlantic Ocean the underestimated values (around -10 Wm^{-2}) are predominant.

Figure 6 shows the mean seasonal albedo for the observations (CLARA2), the RegCM4 model and the differences between them. As can be seen in Fig. 6c, f, i, l, the modeled albedo is overestimated in all the seasons over the eastern and southern parts of SA and oceans. Over the oceans, the overestimated values are higher (lower) than 0.25 in the austral autumn and winter (austral summer and spring). The RegCM4 performs better to represent the albedo in

Fig. 5 As in Fig. 3, but for the net longwave radiation at surface (Wm^{-2})

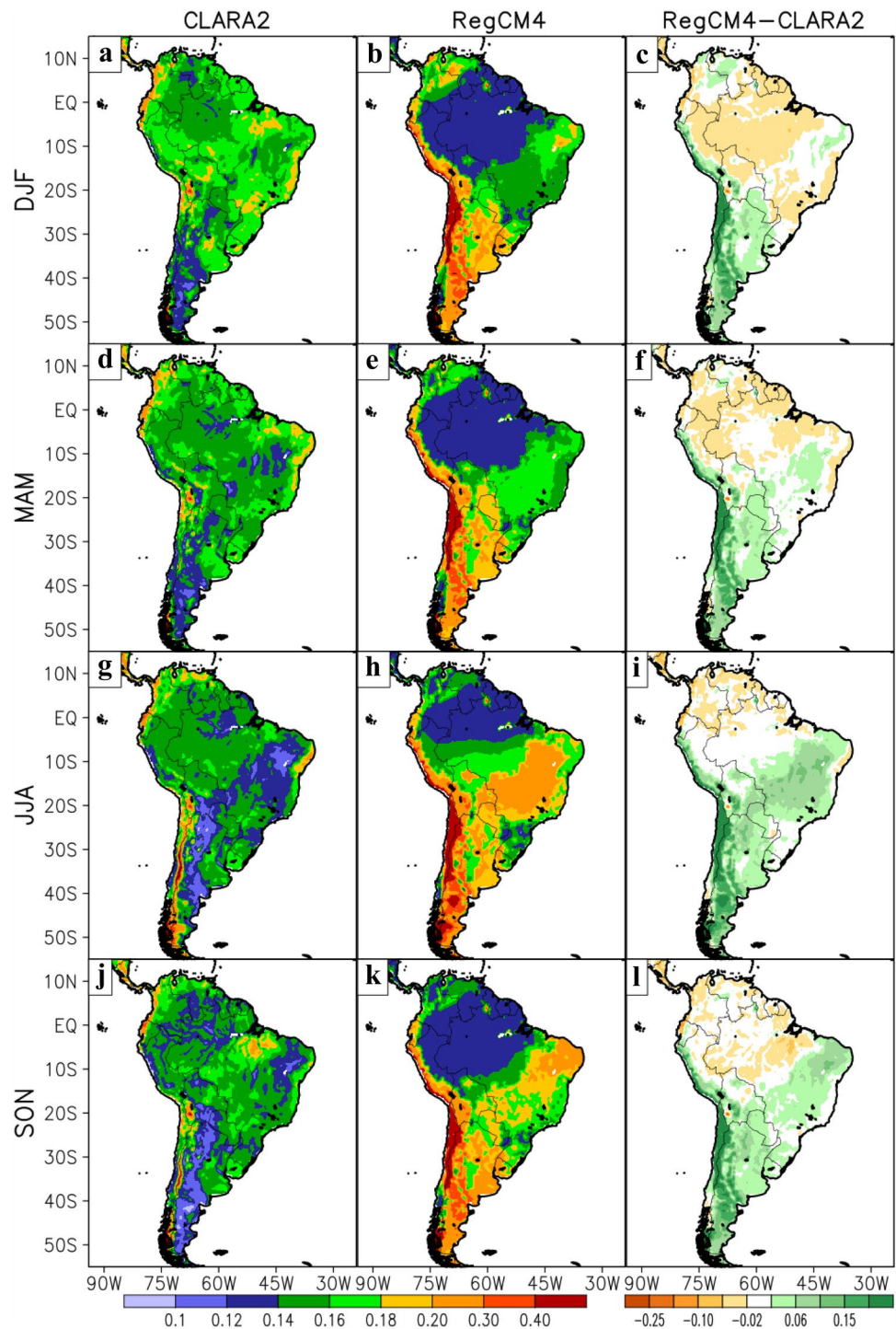


the continental regions, although some parts of the Andes region where the Atacama Desert and other deserts (Paracas, Sechura, etc.) are located, the modeled values are overestimated (higher than 0.25). A feature of the deserts is that the albedo varies from 0.3 to 0.45 (Rechid et al. 2009; Riihela et al. 2013). It can be seen in Fig. 6a that the CLARA2 data underestimated the albedo values in these areas. This may be due to the deficiency of the

CLARA2 instruments that incorrectly calculate the heterogeneity of the near-infrared reflectance near the pixel scales of CLARA2 (Karlsson et al. 2017).

On the other hand, the RegCM4 overestimated values in these deserts due probably to the fact that the BATS scheme was calibrated using values of albedo of North America (Dickinson et al. 1993). It may be taken into account that the RegCM4 albedo is prescribed considering

Fig. 6 As in Fig. 3, but for the surface albedo



the type of soil cover so that in the continental region the albedo values show a better distribution by the kind of vegetation cover than in CLARA2. In the Amazon basin the RegCM4 simulates well the characteristic albedo of the rainforest during the year (values of 0.09–0.16). In the austral autumn, winter and spring, the modeled values are overestimated in the east SA (values higher than 0.15 in

the austral winter). This may be due to the higher RegCM4 reflectance of the vegetation cover in this region.

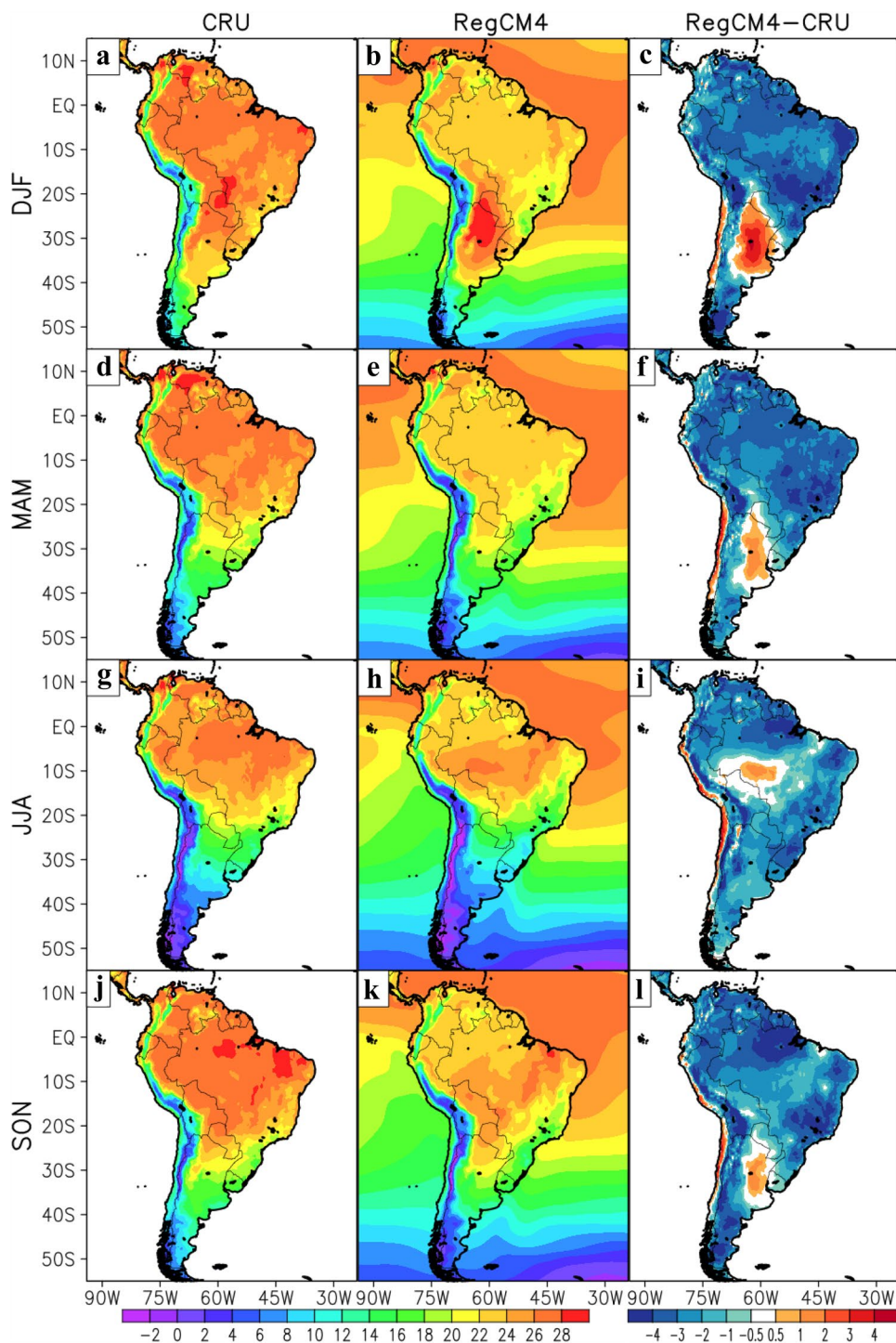
Figure 7 shows the temperature at 2 m above the surface (T_{2m}) over SA for 1982–2012 from CRU data. RegCM4 simulations and the difference between them. T_{2m} is the result of the net of radiation (SW and LW). Thus, it is a very important climate variable due to its influence on the atmospheric

processes. According to its latitudinal and seasonal variation, the earth's surface absorbs SW radiation for about 9–12 h. As can be seen in Fig. 7a, in the austral summer, northward from 30° S, in the regions where the altitude is lower than 750 m, both CRU and RegCM4 simulation show higher values of T_{2m} . However, the RegCM4 underestimated T_{2m} in almost the entire SA continent (values between -0.5 and -4.0 °C). The lower values are located in the central

and south Andes. Otherwise, in the north Argentina T_{2m} is overestimated, with values higher than 2 °C (Fig. 7c). In this region, which are part of the La Plata basin, several models show the same bias (Reboita et al. 2014; Chou et al. 2014).

In the austral winter, the RegCM4 model shows the same deficiency to represent the spatial distribution of T_{2m} as in the case of the austral summer. The values of T_{2m} are underestimated in most of SA, with the higher values in the Andes

Fig. 7 As in Fig. 3, but for 2 m air temperature (°C)



region. On the other hand, there is an overestimation of T_{2m} in the central SA (values between +0.5 and +2.0 °C). This is a common characteristic of the different versions of the RegCM4. In the austral autumn and spring, the RegCM4 simulations show a better performance compared to the austral summer and winter. However, in the north Argentina, the overestimated values (lower than +1 °C) are noted, while in some parts of SA there are underestimated values from -0.5 to -4.0 °C. The underestimated values in most of SA may be associated with the higher values of albedo and CFC simulated by the RegCM4 in the different seasons, as seen in Figs. 3 and 6, respectively.

3.3 Hydrological Cycle

Figure 8 shows the mean seasonal precipitation from CRU/PERSIANN, RegCM4 simulations, and the difference between them for the period 1982–2012. In the austral summer, the position of the ITCZ is well simulated by the RegCM4 compared with CRU data, despite in some areas overestimated and underestimated values are noted (Fig. 8c). The model is also capable to simulate the SACZ, although its position is shifted southwards. This may be due to the fact that modeled low-level winds are stronger than the observations so that the SACZ is displaced southwards due to the more intense winds in the northeast of the system, as shown in Fig. 2. Otherwise, the SA region is strongly influenced by the adjacent oceans that modulate the different atmospheric interactions, especially those associated with the large scale (Yoon and Zeng 2010; Erfanian and Wang 2018; Wang 2019). Erfanian and Wang (2018) pointed out that the CORDEX domain is not able to adequately represent large-scale processes (for example, teleconnections) in the SA and the adjoining oceans (Pacific and Atlantic). On the other hand, they showed that a larger domain than CORDEX allow us a better representation of the location and intensity of the rainy and dry regions in AS.

In the other seasons, it can be seen that the RegCM4 is capable to reproduce the northward and southward movement of the ITCZ according to the season, following the seasonal heating of the oceans in each season. However, the branch of the ITCZ located in the region of Pacific Ocean shows underestimated values of precipitation in all the seasons. This may be associated with the RegCM4 dynamics where the stronger than observed winds displace the moisture flux that favors the precipitation in this region (Fig. 2c, f). In austral autumn, the ITCZ starts to return northwards. Consequently, the higher precipitation rates in the SA continent are located northward of 12° S. While in austral winter, as the ITCZ reaches its position northwards the high precipitation rates in SA continent are placed northward from 6° S (see Fig. 8b). The position of the precipitation maxima in

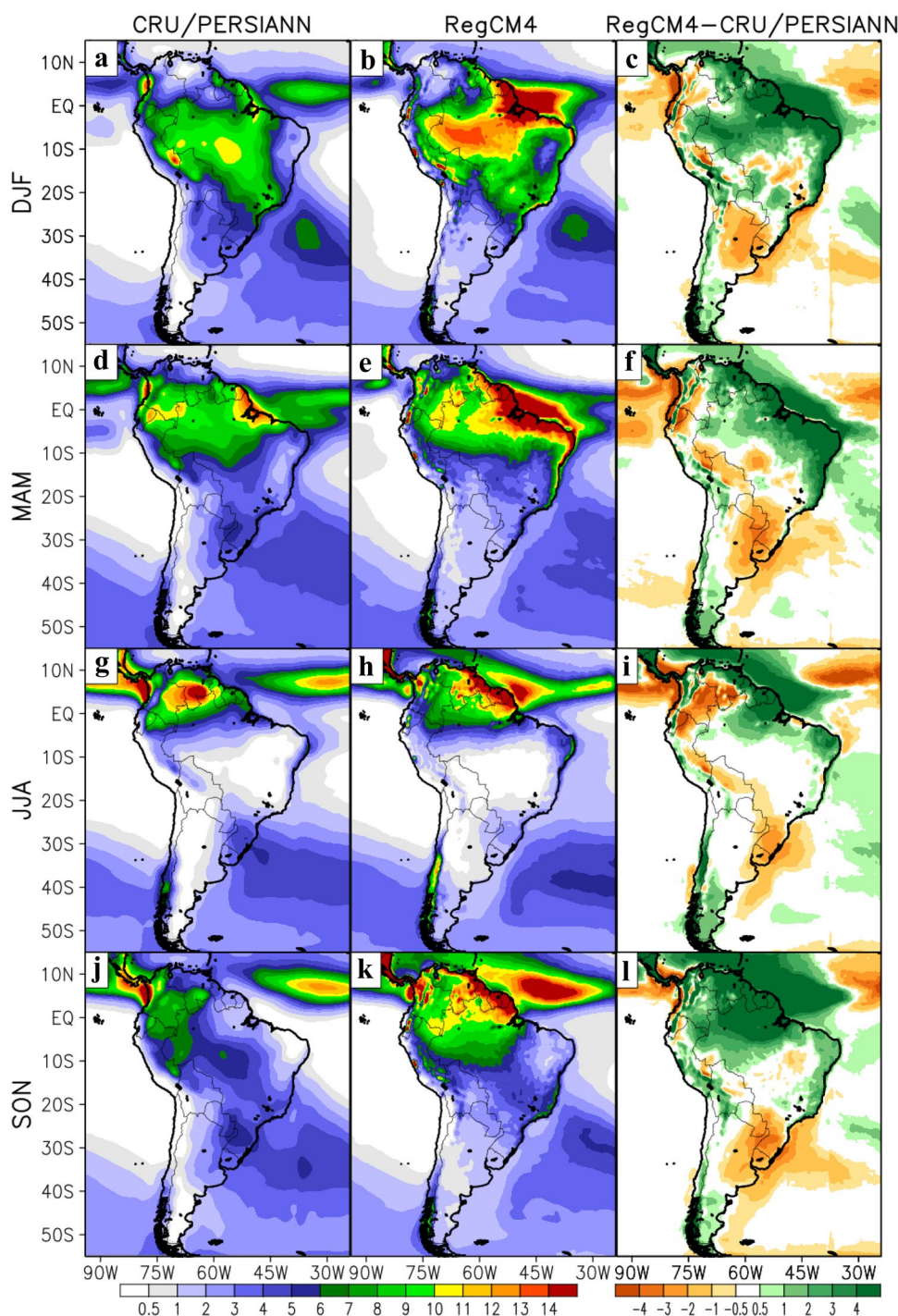
SA simulated by the RegCM4 is similar to those in earlier studies (Garreaud et al. 2009; Reboita et al. 2010).

In the austral spring, the regions of SA with higher precipitation rates are placed northward of 10° S because of the displacement of the ITCZ southwards. However, the RegCM4 has a tendency to underestimate the values of the precipitation rates besides showing a larger extension of the ITCZ. This is related to the fact that in the CRU data the precipitation maxima are located in the northwest SA, while in the RegCM4 simulation they cover the entire region. In the southern La Plata basin, a higher frequency of frontal systems occurs in the austral autumn, winter, and spring (Fig. 8d, g, j), where the austral winter is the season with highest number of cold fronts (Andrade and Cavalcanti 2004; Cardozo et al. 2015). This contributes to the high precipitation rates in the region. As shown by de Jesus et al. (2016), the frontal system contributes with more than 84% of precipitation rates in this region. Nevertheless, the RegCM4 underestimates the values when compared to CRU data (Fig. 8f, i, l). The underestimated values exhibited in these regions are in agreement with the results of de Jesus et al. (2016), which showed that the inaccuracy of precipitation by RegCM4 varies between -25% in summer up to -36% in spring. This is a problem noted in the different available configurations of the RegCM4, which show deficiencies in these areas (da Rocha et al. 2012; Reboita et al. 2014; de Jesus et al. 2016).

The difference between the precipitation and the potential evapotranspiration ($P - PET$) is the net water flux from the atmosphere to the earth's surface (Swenson and Wahr 2006). So, it is taken as a measure of the water availability of the terrestrial hydrological cycle (Greve and Seneviratne 2015), providing a measure of the hydric stress. Particularly, in the Amazon forest the evapotranspiration plays an important role in the surface-atmosphere interaction processes since it is the mechanism by which large water amounts are transported to the atmosphere, thus contributing to the precipitation rates in the region.

As shown in Fig. 9a, in the austral summer the CRU data present negative maximum values of $P - PET$ over the Andes mountains between 55° S–20° S, with magnitude up to -6 mm day⁻¹ in the southward part and with lower values in the west between 20° S–4° S. A similar distribution pattern of $P - PET$ in the austral spring is observed. This is in agreement with Figs. 3 and Fig. 4, which show that these regions receive large amounts of SW due to the low CFC, allowing that the surface absorbs a higher energy amount to heat the several soil layers. Thus, the values of precipitation are low so that PET is dominant. As can be seen in Fig. 9b, the RegCM4 is capable to simulate the spatial pattern of $P - PET$ in these areas, although with lower spatial extension and weaker negative values. This is due to fact that

Fig. 8 Seasonal climatology (1982–2012) of precipitation (mm day^{-1}) over South America in CRU/PERSIANN (left column), RegCM4 (middle column) and the difference RegCM4 minus CRU/PERSIANN (right column)



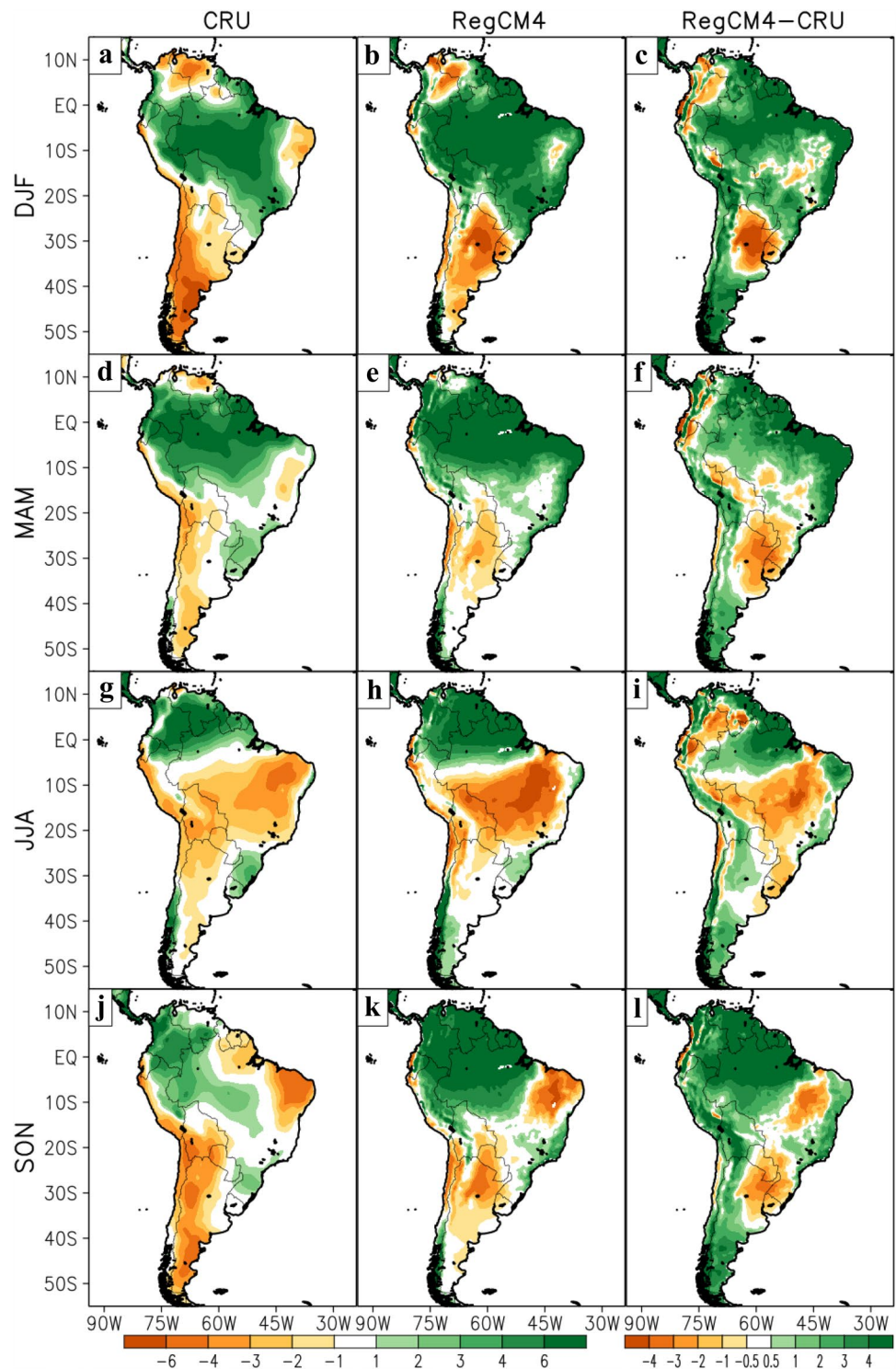
the RegCM4 simulations present higher precipitation values (Fig. 8b, c).

Moreover, in these areas T_{2m} is underestimated (Fig. 7c). As can be seen in Fig. 9a, in the austral summer, the north SA region also presents negative $P - PET$ values, showing that PET is dominant due to the low CFC and high SW. In the RegCM4 simulation a similar pattern is obtained, though with higher PET values. Another region with dominant PET values is observed in the semiarid northeast Brazil. From

Fig. 9a, b, d, e, it can be noted that in the austral summer and autumn the extension of the negative $P - PET$ is smaller in RegCM4 simulations than in CRU data, while the opposite occurs in the austral spring (Fig. 9j, k).

The continental dry season occurs in the austral winter, particularly in the central SA, where negative $P - PET$ values are observed as a response to the low CFC and high T_{2m} (Figs. 3, 7, respectively). The negative values of $P - PET$ are more intense in the east side of central SA in the

Fig. 9 The same as in Fig. 8, but for the precipitation minus potential evapotranspiration (P-PET) (mm day^{-1})



RegCM4 simulations, as shown in Fig. 9c. This is because the RegCM4 overestimates the observed T_{2m} (Fig. 7c). In the austral winter, the distribution pattern of $P - PET$ is similar to the other seasons. However, the $P - PET$ values are positive between $50^{\circ} S$ and $30^{\circ} S$ in the west side of the Andes (Fig. 9g). This is due to the higher frequency of frontal systems reaching the region in the wintertime (Carvalho et al.

2004) which, in crossing the mountain, cause the increase of precipitation in the west side of the cordillera. Moreover, in this season the south Pacific high is located close to the continent contributing to the occurrence of precipitation. The RegCM4 simulation presents a larger (smaller) territorial and latitudinal extension of the positive (negative) values of $P - PET$ in the region of the Andes mountains. Similar to

the other seasons, in the Andes region the RegCM4 shows underestimated and overestimated values of $P - PET$, however the RegCM4 errors may be due to SW and P biases in this area.

The observed positive $P - PET$ values over SA follow the seasonal distribution of precipitation, where in the austral summer the ITCZ and SACZ are the principal systems that contribute to the high precipitation rates (Fig. 9a). Even though the SW is high, the high values of CFC significantly reduce the SW that reaches the surface and thus the SW values do not play a significant role in the PET processes. In these regions, the main contribution to the convective processes is due to the moisture transported by the tropical Atlantic trade winds (Drumond et al. 2008; Duran-Quesada et al. 2009; Zemp et al. 2017). In the austral autumn, the ITCZ displaces northwards so that the positive values of $P - PET$ are located to the north of $20^\circ S$ (Fig. 9d). However, the RegCM4 simulated values are higher than the observed 4 mm day^{-1} , as shown in Fig. 9e, f.

In the austral winter, there are negative values of $P - PET$ in the central SA due to the movement of the ITCZ northwards and areas with positive values located to the north of $5^\circ S$ (Fig. 9g). As shown in Fig. 9h, the simulation of the RegCM4 is in a good agreement with the observations,

although overestimated and underestimated values can be seen. In the austral spring, as the ITCZ starts to return southwards so that the positive values of $P - PET$ are located in the northwest and parts of the central SA (Fig. 9j), while in the RegCM4 simulation the positive values appear in the entire north and some parts of SA (Fig. 9k).

3.4 Annual Cycle Variability

Figure 10 shows the box-plot for the annual cycle of precipitation, surface net radiation (SW minus LW) and T_{2m} to period of analysis. As can be seen, precipitation simulated by the RegCM4 is overestimated in the regions of Amazon and northeast Brazil, mainly in the austral summer and spring months, while in the other months the simulated values are close to those in CRU data. On the other hand, it is noted that in the Amazon region the variability of precipitation simulated by the RegCM4 shows an interannual distribution similar to that in CRU data, confirming the model good performance in this region (Fig. 8). In the region of the northeast Brazil, the interannual distribution of precipitation is also well represented by the RegCM4, with little variability in July and September and higher variability in the other months. The high overestimated values (with

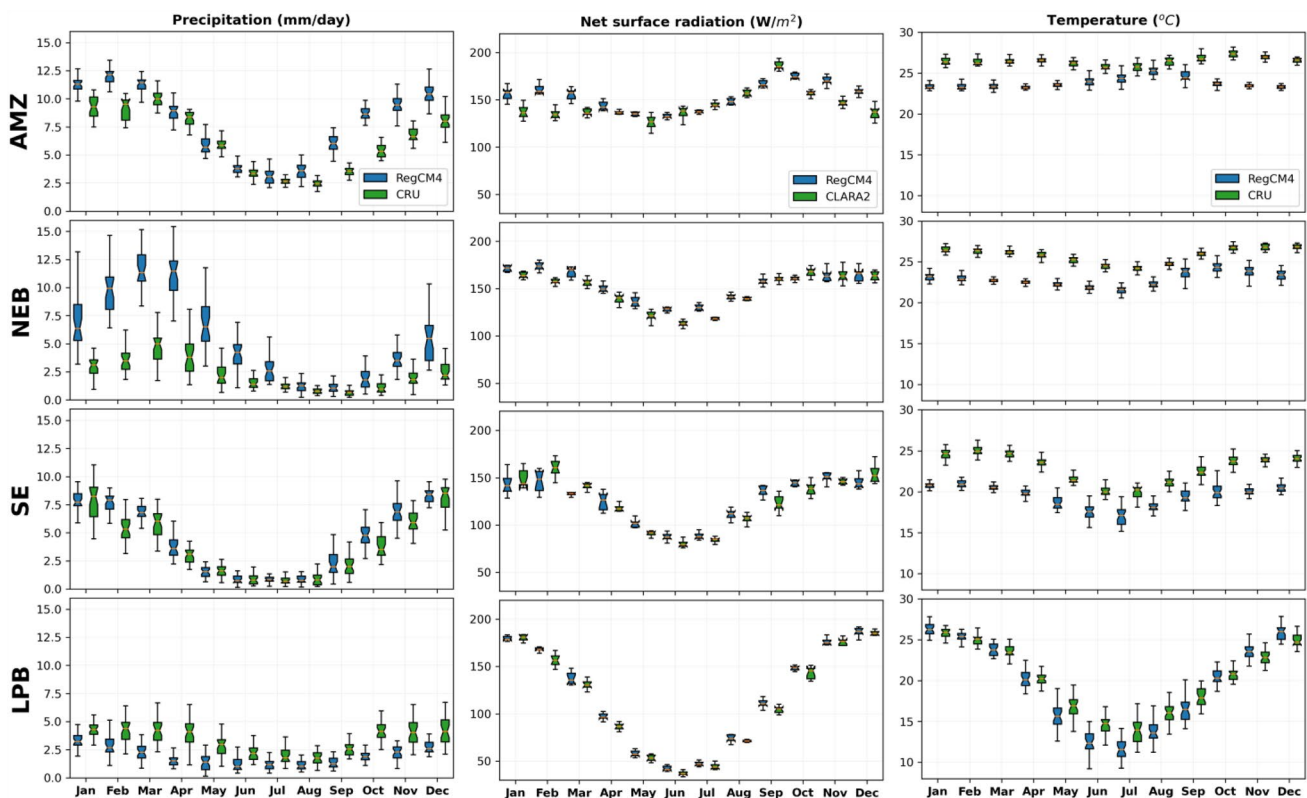


Fig. 10 Box-plot for the annual cycle of precipitation (mm day^{-1}), net surface radiation (Wm^{-2}) and temperature 2 m ($^\circ\text{C}$) over Amazon (AMZ), Northeast Brazil (NEB), Southeast Brazil (SE) and La Plata Basin (LPB) regions to period of analysis

precipitation rates similar to those in the Amazon region) is due to the fact that the RegCM4 is not able to simulate the precipitation rates in the regions with ocean-surface contrast, as can be seen in the third column of Fig. 8. This is a problem of regional models (Giorgi and Gutowski 2015). In the regions of the southeast Brazil and La Plata basin, the RegCM4 performs better the interannual variability of precipitation, showing simulated values in good agreement with those in CRU data. In the four regions, the RegCM4 shows better performance in the months from May to September. The interannual variability of surface net radiation is in a good agreement with CLARA2. Also, the biases are lower than those in Figs. 3 and 4. It can be noted that in La Plata basin region there is a larger amplitude: the maxima (around 185 Wm^{-2}) and minima (around 30 Wm^{-2}). In the other three regions, the surface net radiation varies between 110 and 190 Wm^{-2} , each region showing own maxima and minima because of their different meteorological conditions.

At last, it is noted that in the regions of Amazon, northeast Brazil and southeast Brazil T_{2m} is underestimated along the year, even thus the RegCM4 reproduces well the interannual variability observed in CRU data. In addition, the amplitude of the interannual variability in the regions of Amazon and northeast Brazil is similar, varying between 22 and $28 \text{ }^\circ\text{C}$, while in the southeast Brazil it varies between 16 and $26 \text{ }^\circ\text{C}$. The better performance of the model in simulating the interannual variability is for La Plata basin region, showing amplitudes from 10 to $27 \text{ }^\circ\text{C}$. The results presented for the Amazon region is similar to those in Lange et al. (2015), however the simulation in the present study shows lower biases.

4 Discussion

The analysis carried out on the surface radiative balance and the hydrological cycle indicate that CFC plays a very important role in both analyzed components. It is noted that the regions with higher values of CFC are higher precipitation rates areas, as well as with lower SW at the surface and LW emitted to space occur. While in the regions with lower CFC values the opposite occurs (Figs. 2, 3, 4, 8). Undoubtedly, clouds are one of the most relevant components of the atmosphere system (Stephens 2005; Henderson et al. 2013; Matus and L'Ecuyer 2017), providing one of the strong climate feedback mechanisms (Stephens 2005; Soden and Vecchi 2011). The biases in CFC during the months of austral summer and winter are lower than those in Pessacg et al. (2014) and Lange et al. (2015), with values lower than 30%. As well as, the simulation in the oceanic regions is better than that in Pessacg et al. (2014) and Lange et al. (2015), although the values are higher than 30%. Moreover, the cloud microphysics needs to be improved, mainly in the

oceanic regions, where the RegCM4 shows poor performance. Regarding the microphysical mechanisms for cloud feedback, significant uncertainties still remain (Gettelman and Sherwood 2016). To reduce the biases in CFC simulation in the RegCM4 the methodologies of Lange et al. (2015) and Brisson et al. (2016) may be used. This may be subject for a forthcoming study.

Pessacg et al. (2014) and Chiacchio et al. (2015) showed that the SW and LW are strongly influenced by CFC, albedo and T_{2m} . This is in agreement with the results presented in Figs. 2, 5 and 6, where is noted that in the regions with lower biases of these variables the SW and LW are better represented. On the other hand, the albedo directly affects the radiation flux that is absorbed by different types of surface, where the vegetation and oceans have low albedo. The RegCM4 simulations show albedo values relatively higher (lower) than the observed to the south (north) of 20° S , with higher values of + (–) 0.01. These albedo biases are mainly associated with the fact that the albedo is parameterized considering each type of surface and does not adequately represent their annual variability. The overestimated albedo in the RegCM4 causes lower values of T_{2m} northward of 20° S over the SA continent. This is because of the higher albedo reflects more SW, so that there is lower amount of energy to heat the surface. Also, the underestimated T_{2m} southward of 20° S and in other regions of SA can be associated with the BATS scheme used in the present study, which calculates the soil temperature by force-restore method (Giorgi et al. 2012) that splits the ground into two layers to approximate the surface energy budget. Over the oceans, higher values of albedo are also noted. However, the surface energy deficit may be compensated by a high amount of SW reaching the surface due to the lower CFC. However, the errors in T_{2m} in regional models have lower impact (lower than 10%) than the errors in LW (Pessacg et al. (2014). Pessacg et al. (2014) and Kothe et al. (2011) showed that the errors in SW and LW are mainly due to the uncertainties in CFC. The errors in SW and LW presented in Figs. 3 and 4 are relatively lower than, or in some cases equal to, those in earlier studies over SA, Europe, and north Africa (Pessacg et al. 2014; Kothe et al. 2011; Chiacchio et al. 2015; Panitz et al. 2014). The main sources of uncertainties may be associated with the configurations of the models and the geographic influence. Many dynamical, physical, and biologic processes that occur in the surface are a direct response to the SW and LW radiative fluxes. Thus, a good representation of SW and LW fluxes in regional and global models is essential.

The hydrological cycle is an essential geophysical process that provides continuous distribution of water between the different components of the climate system. Therefore, a good representation of precipitation is important to better understand the different processes that occur in the diverse phenomena of the atmospheric system. In most of SA, it is

noted that in the regions with higher values of CFC (Fig. 3) there is an occurrence of high precipitation rates (Fig. 8). Thus, a good representation of CFC, as well as the cloud microphysics processes, will improve the simulation of the precipitation rates. In addition, a good representation of the dynamic of the regional circulation is important due to the fact that it permits a good simulation of the atmospheric systems in the different parts of SA. On the other hand, the RegCM4 deficiencies in intensity and temporal evolution of precipitation, mainly in the central and southern Amazon, are associated with the selected domain (Erfanian and Wang 2018), which fails to properly represent the adjoining oceans teleconnection processes. In northern and northeast parts, the differences are associated with deficiencies of RegCM4 in representing precipitation rates. It must be taken into account that the global and regional models have yet deficiencies to represent the nonlinear relationship between SST and precipitation over tropical regions so that overestimated or underestimated modeled precipitation rates may be noted (Coppola et al. 2012; Flato et al. 2014; Zhang et al. 2015). In addition, the deficiencies in representing the precipitation in the southeastern SA (see Fig. 8) would be associated with the poor representation of the cyclogenesis by RegCM model (Reboita et al. 2018a, b). The bias of precipitation rates over the Andes region may be associated with the deficiencies of regional models to represent satisfactorily the intensity of the winds in mountain slopes due to their abrupt changes (see Fig. 2). As a consequence, the microphysics processes are affected and, in general, lead to the overestimation of precipitation in the summer months (the winds carry moisture from Amazon to the Andes). In addition, recent studies have shown that regional models have some deficiencies in representing the diurnal cycle (Bechtold et al. 2004; Lange et al. 2015; Ou et al. 2020). This is another important factor that may influence the performance of the model simulation of precipitation. Evidently, improvements in cloud representation will allow us to better depict the spatial and temporal precipitation rates in regional and global simulations.

5 Conclusion

In this paper, we conducted a 34-long year transient simulation to assess the ability of the RegCM4 to represent the surface radiative balance and the hydrological cycle over the CORDEX SA domain.

The RegCM4, in general, was able to reproduce the main patterns of the observed seasonal variables associated with the surface radiative balance and hydrological cycle. However, some differences were noted. The RegCM4 overestimated the variables associated with the radiative balance (CFC, SW, LW and albedo), mainly over

the oceans, in all the seasons. The net surface SW and LW errors were associated to the errors in the CFC due to the inaccuracy of the model in representing the low-level clouds, which is predominant in the regions of the Pacific Ocean near to Peru and Chile as well as most part of the south Atlantic ocean (Boucher et al. 2013). It must be pointed out that the CFC plays an important role in modulating the net surface radiation. Besides, the albedo was not well simulated by the model which contributes to the errors in SW and LW.

The RegCM4 simulations of the hydrological cycle variables also presented differences compared with the observations. Although the position of the ITCZ in the austral summer was well simulated by the RegCM4, in some areas, overestimated and underestimated values were noted. In the other seasons, the RegCM4 was capable of reproducing the northward and southward movement of the ITCZ, according to the seasonal heating of the oceans. However, over the Pacific Ocean the seasonal warming was underestimated, which may be associated with the RegCM4 dynamics where stronger than observed winds shift the position of the moisture flux that sustain the precipitation in this region. Some deficiencies in the model simulations may be associated with the CORDEX domain, which fails to adequately represent the oceanic processes that influence the SA climate (Erfanian and Wang, 2018).

It is clear that simulation of surface temperature has to be improved to better represent evapotranspiration, which is an important component of the hydrological cycle since it transfers soil moisture to the atmosphere. In addition, the cloud cover fraction also needs to be improved to reduce the biases in precipitation, PET, and the radiative surface fluxes SW and LW. To reduce the deficiencies in the model simulations, new physical schemes have been implemented in RegCM4. For example, the scheme of the University of Washington which gives a better simulation of the low cloudiness and the complex microphysics scheme (hydrometeors) (Nogherotto et al. 2016) is recently implemented into RegCM4. Also, the Community Land Model (CLM) surface scheme may be used to obtain a better simulation of temperature and surface radiative balance, as shown by Reboita et al. (2014). The use of these schemes may be the subject of forthcoming study.

Acknowledgements This paper makes part of the Ph.D. Thesis of the first author. The first author is thankful to CAPES (Coordenação de Aperfeiçoamento de Pessoal de Nível Superior) for the studentship resources. The authors are thankful to the four anonymous reviewers for their useful suggestions and comments.

Declarations

Conflict of interest The author declares no known competing financial interests or personal relationships that could have appeared to influence the work reported in this paper.

Open Access This article is licensed under a Creative Commons Attribution 4.0 International License, which permits use, sharing, adaptation, distribution and reproduction in any medium or format, as long as you give appropriate credit to the original author(s) and the source, provide a link to the Creative Commons licence, and indicate if changes were made. The images or other third party material in this article are included in the article's Creative Commons licence, unless indicated otherwise in a credit line to the material. If material is not included in the article's Creative Commons licence and your intended use is not permitted by statutory regulation or exceeds the permitted use, you will need to obtain permission directly from the copyright holder. To view a copy of this licence, visit <http://creativecommons.org/licenses/by/4.0/>.

References

- Almazroui M, Islam MN, Alkhalaf AK, Saeed F, Dambul R, Rahman MA (2016) Simulation of temperature and precipitation climatology for the CORDEX-MENA/Arab domain using RegCM4. *Arab J Geosci* 9(1):1–14
- Andrade KM, Cavalcanti IFA (2004) Climatologia dos sistemas frontais e padrões de comportamento para o verão na América do Sul. In: *Anais, Congresso Brasileiro de Meteorologia*, 13, SBMET. <http://urlib.net/rep/cptec.inpe.br/walmeida/2004/09.21.13.45>
- Arraut JM, Satyamurty P (2009) Precipitation and water vapor transport in the southern hemisphere with emphasis on the South American region. *J Appl Meteorol Climatol* 48(9):1902–1912. <https://doi.org/10.1175/2009JAMC2030.1>
- Ashouri H, Hsu KL, Sorooshian S, Braithwaite DK, Knapp KR, Cecil LD, Nelson BR, Prat OP (2015) PERSIANN-CDR: daily precipitation climate data record from multisatellite observations for hydrological and climate studies. *Bull Am Meteor Soc* 96(1):69–83
- Bechtold P, Chaboureaud JP, Beljaars A, Betts A, Köhler M, Miller M, Redelsperger JL (2004) The simulation of the diurnal cycle of convective precipitation over land in a global model. *Quart J R Meteorol Soc J Atmos Sci Appl Meteorol Phys Oceanogr* 130(604):3119–3137. <https://doi.org/10.1256/qj.03.103>
- Boucher O, Randall D, Artaxo P, Bretherton C, Feingold G, Forster P, Kerminen VM, Kondo Y, Liao H, Lohmann U et al (2013) Clouds and aerosols. In: *Climate change 2013: the physical science basis. Contribution of Working Group I to the Fifth Assessment Report of the Intergovernmental Panel on Climate Change*, Cambridge University Press, pp 571–657
- Brisson E, Van Weverberg K, Demuzere M, Devis A, Saeed S, Stengel M, van Lipzig NP (2016) How well can a convection-permitting climate model reproduce decadal statistics of precipitation, temperature and cloud characteristics? *Clim Dyn* 47(9):3043–3061
- Cardozo AB, Custódio IS, Reboita MS, Garcia SR (2015) Climatologia de frentes frias na América do Sul e sua relação com o modo anular sul (Climatology of cold fronts over South America and its relation with the southern annular mode). *Revista Brasileira de Climatologia*, 17. <https://doi.org/10.5380/abclima.v17i0.40124>
- Carvalho LM, Jones C, Liebmann B (2004) The South Atlantic Convergence Zone: intensity, form, persistence, and relationships with intraseasonal to interannual activity and extreme rainfall. *J Clim* 17(1):88–108. [https://doi.org/10.1175/1520-0442\(2004\)017<0088:TSACZI>2.0.CO;2](https://doi.org/10.1175/1520-0442(2004)017<0088:TSACZI>2.0.CO;2)
- Chen TC (1985) Global water vapor flux and maintenance during FGGE. *Mon Weather Rev* 113(10):1801–1819. [https://doi.org/10.1175/1520-0493\(1985\)113<1801:GWVFAM>2.0.CO;2](https://doi.org/10.1175/1520-0493(1985)113<1801:GWVFAM>2.0.CO;2)
- Chiacchio M, Solmon F, Giorgi F, JRP S, Wild M (2015) Evaluation of the radiation budget with a regional climate model over Europe and inspection of dimming and brightening. *J Geophys Res Atmos* 120(5):1951–1971
- Chou SC, Marengo JA, Lyra AA, Sueiro G, Pesquero JF, Alves LM, Kay G, Betts R, Chagas DJ, Gomes JL, Bustamante JF, Tavares P (2012) Downscaling of South America present climate driven by 4-member HadCM3 runs. *Clim Dyn* 38(3–4):635–653. <https://doi.org/10.1007/s00382-011-1002-8>
- Chou SC, Lyra A, Mourão C, Dereczynski C, Pilotto I, Gomes J, Bustamante J, Tavares P, Silva A, Rodrigues D, Campos D, Chagas D, Sueiro G, Siqueira G, Nobre P, Marengo JA (2014) Evaluation of the eta simulations nested in three global climate models. *Am J Clim Change* 3(05):438. <https://doi.org/10.4236/ajcc.2014.35039>
- Coppola E, Giorgi F, Mariotti L, Bi X (2012) RegT-Band: a tropical band version of RegCM4. *Clim Res* 52:115–133. <https://doi.org/10.3354/cr01078>
- Culf AD, Esteves JL, Marques-Filho ADO, Rocha HD (1996) Radiation, temperature and humidity over forest and pasture in Amazonia. In: Gash JHC, Nobre CA, Roberts JM, Victoria RL (eds) *Amazonian deforestation and climate*. p 175–191
- da Rocha HR, Manzi AO, Cabral OM, Miller SD, Goulden ML, Saleska SR, Coupe NR, Wofsy SC, Borma LS, Artaxo P et al (2009) Patterns of water and heat flux across a biome gradient from tropical forest to Savanna in Brazil. *J Geophys Res Biogeosci*. <https://doi.org/10.1029/2007JG000640>
- da Rocha RP, Cuadra SV, Reboita MS, Kruger LF, Ambrizzi T, Krusche N (2012) Effects of regcm3 parameterizations on simulated rainy season over South America. *Clim Res* 52:253–265. <https://doi.org/10.3354/cr01065>
- de Almeida VA, Marton E, Nunes AMB (2018) Assessing the ability of three global reanalysis products to reproduce South American monsoon precipitation. *Atmósfera* 31(1):1–10. <https://doi.org/10.20937/atm.2018.31.01.01>
- de Jesus EM, da Rocha RP, Reboita MS, Llopart M, Dutra LMM, Remedio ARC (2016) Contribution of cold fronts to seasonal rainfall in simulations over the southern La Plata basin. *Clim Res* 68(2–3):243–255. <https://doi.org/10.3354/cr01358>
- Dee DP, Uppala SM, Simmons AJ, Berrisford P, Poli P, Kobayashi S, Andrae U, Balmaseda MA, Balsamo G, Bauer P et al (2011) The ERA-Interim reanalysis: configuration and performance of the data assimilation system. *Q J R Meteorol Soc* 137(656):553–597. <https://doi.org/10.1002/qj.828>
- Dickinson E, Henderson-Sellers A, Kennedy J (1993) Biosphere-atmosphere transfer scheme (BATS) version 1e as coupled to the NCAR community climate model. NCAR Tech Note TH-387 + STR, p 80
- Drumond A, Nieto R, Gimeno L, Ambrizzi T (2008) A Lagrangian identification of major sources of moisture over Central Brazil and La Plata Basin. *J Geophys Res Atmos*. <https://doi.org/10.1029/2007JD009547>
- Duran-Quesada AM, Reboita M, Gimeno L, Nieto R (2009) The role of the tropics in the global water cycle: precipitation and moisture transport in tropical America. *ESASP* 674:34
- Emanuel KA, Zivkovic-Rothman M (1999) Development and evaluation of a convection scheme for use in climate models. *J Atmos Sci* 56(11):1766–1782. [https://doi.org/10.1175/1520-0469\(1999\)056<1766:DAEOAC>2.0.CO;2](https://doi.org/10.1175/1520-0469(1999)056<1766:DAEOAC>2.0.CO;2)
- Erfanian A, Wang G (2018) Explicitly accounting for the role of remote oceans in regional climate modeling of South America. *J Adv Model Earth Syst* 10(10):2408–2426. <https://doi.org/10.1029/2018MS001444>

- Fahad AA, Burls NJ, Swenson ET, Straus DM (2021) The influence of South Pacific Convergence Zone heating on the South Pacific Subtropical Anticyclone. *J Clim* 34(10):3787–3798
- Fernandez J, Franchito SH, Rao VB (2006) Simulation of the summer circulation over South America by two regional climate models. Part I: Mean climatology. *Theor Appl Climatol* 86:247–260. <https://doi.org/10.1007/s00704-005-0212-6>
- Flato G, Marotzke J, Abiodun B, Braconnot P, Chou SC, Collins W, Cox P, Driouech F, Emori S, Eyring V et al (2014) Evaluation of climate models. In: *Climate change 2013: the physical science basis. Contribution of Working Group I to the Fifth Assessment Report of the Intergovernmental Panel on Climate Change*, Cambridge University Press, pp 741–866
- Franchito SH, Fernandez JPR, Pareja D (2014) Surrogate climate change scenario and projections with a regional climate model: impact on the aridity in South America. *Am J Clim Change* 3(05):474. <https://doi.org/10.4236/ajcc.2014.35041>
- Garreaud RD, Christie D, Barichivih J, Maldonado A (2007) The climate and weather of the west coast of subtropical South America. In: *Fourth international conference on fog collection and dew*, La Serena, Chile, pp 22–27
- Garreaud RD, Vuille M, Compagnucci R, Marengo JA (2009) Present-day South American climate. *Palaeogeogr Palaeoclimatol Palaeoecol* 281(3–4):180–195
- Gottelman A, Sherwood S (2016) Processes responsible for cloud feedback. *Curr Clim Change Rep* 2(4):179–189. <https://doi.org/10.1007/s40641-016-0052-8>
- Giorgi F, Gutowski JWJ (2015) Regional dynamical downscaling and the CORDEX initiative. *Annu Rev Environ Resour* 40:467–490. <https://doi.org/10.1146/annurev-environ-102014-021217>
- Giorgi F, Jones C, Asrar GR (2009) Addressing climate information needs at the regional level: the CORDEX framework. *World Meteorol Organ WMO Bull* 58(3):175
- Giorgi F, Coppola E, Solmon F, Mariotti L, Sylla M, Bi X, Elguindi N, Diro G, Nair V, Giuliani G et al (2012) RegCM4: model description and preliminary tests over multiple CORDEX domains. *Clim Res* 52:7–29. <https://doi.org/10.3354/cr01018>
- Grell GA (1993) Prognostic evaluation of assumptions used by cumulus parameterizations. *Mon Weather Rev* 121(3):764–787. [https://doi.org/10.1175/1520-0493\(1993\)121<0764:PEOAU>2.0.CO;2](https://doi.org/10.1175/1520-0493(1993)121<0764:PEOAU>2.0.CO;2)
- Grell GA, Dudhia J, Stauffer DR (1994) A description of the Fifth-Generation Penn State/Ncar Mesoscale Model (MM5). NCAR Tech TN-398+STR <http://n2t.net/ark:/85065/d7b857g2>
- Greve P, Seneviratne SI (2015) Assessment of future changes in water availability and aridity. *Geophys Res Lett* 42(13):5493–5499. <https://doi.org/10.1002/2015GL064127>
- Harris I, Jones PD, Osborn TJ, Lister DH (2014) Updated high-resolution grids of monthly climatic observations—the cru ts3.10 dataset. *Int J Climatol* 34(3):623–642. <https://doi.org/10.1002/joc.3711>
- Harris I, Osborn TJ, Jones P, Lister D (2020) Version 4 of the CRU TS monthly high-resolution gridded multivariate climate dataset. *Sci Data* 7(1):1–18. <https://doi.org/10.1038/s41597-020-0453-3>
- Henderson DS, L'Ecuyer T, Stephens G, Partain P, Sekiguchi M (2013) A multisensor perspective on the radiative impacts of clouds and aerosols. *J Appl Meteorol Climatol* 52(4):853–871. <https://doi.org/10.1175/JAMC-D-12-025.1>
- Holtlag AAM, De Bruijn EIF, Pan H-L (1990) A high resolution air mass transformation model for short-range weather forecasting. *Mon Weather Rev* 118(8):1561–1575. [https://doi.org/10.1175/1520-0493\(1990\)118<1561:AHRAMT>2.0.CO;2](https://doi.org/10.1175/1520-0493(1990)118<1561:AHRAMT>2.0.CO;2)
- Horel JD, Hahmann AN, Geisler JE (1989) An investigation of the annual cycle of convective activity over the tropical Americas. *J Clim* 2(11):1388–1403. [https://doi.org/10.1175/1520-0442\(1989\)002%3C1388:AOTAC%3E2.0.CO;2](https://doi.org/10.1175/1520-0442(1989)002%3C1388:AOTAC%3E2.0.CO;2)
- Inglezakis V, Pouloupoulos S, Arkhangelsky E, Zorpas A, Menegaki A (2016) Aquatic environment. *Environment and development*. Elsevier, pp 137–212. <https://doi.org/10.1016/B978-0-444-62733-9.00003-4>
- Karlsson KG, Anttila K, Trentmann J, Stengel M, Meirink JF, Devasthale A, Hanschmann T, Kothe S, Jaaskelainen E, Sedlar J et al (2017) CLARA-A2: the second edition of the CM SAF cloud and radiation data record from 34 years of global AVHRR data. *Atmos Chem Phys* 17(9):5809–5828. <https://doi.org/10.5194/acp-17-5809-2017>
- Kiehl T, Hack J, Bonan B, Boville A, Briegleb P, Williamson L, Rasch J (1996) Description of the NCAR community climate model (ccm3). NCAR Tech TN-420+STR. <http://n2t.net/ark:/85065/d70v8c61>
- Kothe S, Dobler A, Beck A, Ahrens B (2011) The radiation budget in a regional climate model. *Clim Dyn* 36(5–6):1023–1036. <https://doi.org/10.1007/s00382-009-0733-2>
- Lange S, Rockel B, Volkholz J, Bookhagen B (2015) Regional climate model sensitivities to parametrizations of convection and non-precipitating subgrid-scale clouds over South America. *Clim Dyn* 44(9–10):2839–2857. <https://doi.org/10.1007/s00382-014-2199-0>
- Llopart M, da Rocha RP, Reboita M, Cuadra S (2017) Sensitivity of simulated South America climate to the land surface schemes in RegCM4. *Clim Dyn* 49(11):3975–3987. <https://doi.org/10.1007/s00382-017-3557-5>
- Llopart MP, Reboita MS, da Rocha RP, Machado JP (2019) Performance do Acoplamento RegCM4.3 e CLM3.5: Uma Análise Sobre o Sudeste do Brasil. *Anuário Do Instituto De Geociências* 41(3):113–124
- Llopart M, Reboita MS, da Rocha RP (2020) Assessment of multi-model climate projections of water resources over South America CORDEX domain. *Clim Dyn* 54(1):99–116. <https://doi.org/10.1007/s00382-019-04990-z>
- Marengo JA (2004) Interdecadal variability and trends of rainfall across the amazon basin. *Theor Appl Climatol* 78(1–3):79–96. <https://doi.org/10.1007/s00704-004-0045-8>
- Marengo JA (2006) On the hydrological cycle of the amazon basin: a historical review and current state-of-the-art. *Revista Brasileira de Meteorologia* 21(3):1–19. <http://urlib.net/rep/6qtX3pFwXQZGivnJUY/PR4yE>
- Martinez JA, Dominguez F (2014) Sources of atmospheric moisture for the La Plata river basin. *J Clim* 27(17):6737–6753. <https://doi.org/10.1175/JCLI-D-14-00022.1>
- Matus AV, L'Ecuyer TS (2017) The role of cloud phase in earth's radiation budget. *J Geophys Res Atmos* 122(5):2559–2578. <https://doi.org/10.1002/2016JD025951>
- Montini TL, Jones C, Carvalho LM (2019) The South American Low-Level Jet: a new climatology, variability, and changes. *J Geophys Res Atmos* 124(3):1200–1218
- Nepstad D, Lefebvre P, Lopes da Silva U, Tomasella J, Schlesinger P, Solórzano L, Moutinho P, Ray D, Guerreira Benito J (2004) Amazon drought and its implications for forest flammability and tree growth: a basin-wide analysis. *Glob Change Biol* 10(5):704–717. <https://doi.org/10.1111/j.1529-8817.2003.00772.x>
- Nobre CA, Obregon GO, Marengo JA, Fu R, Poveda G (2009) Characteristics of Amazonian climate: main features. *Amazonia and global change*, edited by: Keller M, Bustamante M, Gash J, Silva Dias P. *Geophys Mon Ser* 186:149–162. <https://doi.org/10.1029/2009GM000903>
- Nogherotto R, Tompkins AM, Giuliani G, Coppola E, Giorgi F (2016) Numerical framework and performance of the new multiple-phase cloud microphysics scheme in RegCM4.5: precipitation, cloud microphysics, and cloud radiative effects. *Geosci Model Dev* 9(7):2533–2547. <https://doi.org/10.5194/gmd-9-2533-2016>

- Ou T, Chen D, Chen X, Lin C, Yang K, Lai HW, Zhang F (2020) Simulation of summer precipitation diurnal cycles over the Tibetan plateau at the gray-zone grid spacing for cumulus parameterization. *Clim Dyn* 54(7):3525–3539
- Pal JS, Small EE, Eltahir EA (2000) Simulation of regional-scale water and energy budgets: representation of subgrid cloud and precipitation processes within RegCM. *J Geophys Res Atmos* 105(D24):29579–29594. <https://doi.org/10.1029/2000JD900415>
- Panitz HJ, Dosio A, Buchner M, Luthi D, Keuler K (2014) COSMO-CLM (CCLM) climate simulations over CORDEX-Africa domain: analysis of the ERA-Interim driven simulations at 0.44 and 0.22 resolution. *Clim Dyn* 42(11–12):3015–3038
- Pereira EB, Martins FR, Gonçalves AR, Costa RS, Lima FJLd, Rütther R, Abreu SLd, Tiepolo GM, Pereira SV, Souza JGd (2017) Atlas brasileiro de energia solar. INPE, São José dos Campos. <http://urlib.net/rep/8JMKD3MGP3W34P/3PERDJE>
- Pessacq NL, Solman SA, Samuelsson P, Sanchez E, Marengo J, Li L, Remedio ARC, Da Rocha RP, Mourão C, Jacob D (2014) The surface radiation budget over South America in a set of regional climate models from the CLARIS-LPB project. *Clim Dyn* 43(5–6):1221–1239. <https://doi.org/10.1007/s00382-013-1916-4>
- Reboita MS, Gan MA, Rocha RPd, Ambrizzi T (2010) Regimes de precipitação na América do Sul: uma revisão bibliográfica. *Revista Brasileira De Meteorologia* 25(2):185–204
- Reboita MS, Fernandez JPR, Llopart MP, da Rocha RP, Pampuch LA, Cruz FT (2014) Assessment of RegCM4.3 over the CORDEX South America domain: sensitivity analysis for physical parameterization schemes. *Clim Res* 60(3):215–234. <https://doi.org/10.3354/cr01239>
- Reboita MS, Amaro TR, de Souza MR (2018a) Winds: intensity and power density simulated by RegCM4 over South America in present and future climate. *Clim Dyn* 51(1–2):187–205
- Reboita MS, da Rocha RP, de Souza MR, Llopart M (2018b) Extratropical cyclones over the southwestern South Atlantic Ocean: HadGEM2-ES and RegCM4 projections. *Int J Climatol* 38(6):2866–2879. <https://doi.org/10.1002/joc.5468>
- Rechid D, Raddatz TJ, Jacob D (2009) Parameterization of snow-free land surface albedo as a function of vegetation phenology based on MODIS data and applied in climate modelling. *Theoret Appl Climatol* 95(3):245–255. <https://doi.org/10.1007/s00704-008-0003-y>
- Riihelä A, Manninen T, Laine V, Andersson K, Kaspar F (2013) CLARA-SAL: a global 28 yr time series of earth's black-sky surface albedo. *Atmos Chem Phys* 13(7):3743–3762. <https://doi.org/10.5194/acp-13-3743-2013>
- Salati E, Marques J (1984) *Climatology of the Amazon region. The Amazon*. Springer, pp 85–126. <https://doi.org/10.1007/978-94-009-6542-3>
- Salati E, Dall'Olio A, Matsui E, Gat JR (1979) Recycling of water in the Amazon basin: an isotopic study. *Water Resour Res* 15(5):1250–1258. <https://doi.org/10.1029/WR015i005p01250>
- Seth A, Rauscher SA, Camargo SJ, Qian JH, Pal JS (2007) RegCM3 regional climatologies for South America using reanalysis and ECHAM global model driving fields. *Clim Dyn* 28:461–480. <https://doi.org/10.1007/s00382-006-0191-z>
- Soden BJ, Vecchi GA (2011) The vertical distribution of cloud feedback in coupled ocean-atmosphere models. *Geophys Res Lett*. <https://doi.org/10.1029/2011GL047632>
- Stephens GL (2005) Cloud feedbacks in the climate system: a critical review. *J Clim* 18(2):237–273. <https://doi.org/10.1175/JCLI-3243.1>
- Sun X, Cook KH, Vizy EK (2017) The south Atlantic subtropical high: climatology and interannual variability. *J Clim* 30(9):3279–3296
- Swenson S, Wahr J (2006) Estimating large-scale precipitation minus evapotranspiration from grace satellite gravity measurements. *J Hydrometeorol* 7(2):252–270. <https://doi.org/10.1175/JHM478.1>
- Wallace JM, Hobbs PV (2006) *The earth system*. In: Wallace JM, Hobbs PV (eds) *Atmospheric science*, 2nd edn. Academic Press, San Diego, pp 25–61
- Wang C (2019) Three-ocean interactions and climate variability: a review and perspective. *Clim Dyn* 53(7):5119–5136
- Yoon JH, Zeng N (2010) An Atlantic influence on amazon rainfall. *Clim Dyn* 34(2–3):249–264. <https://doi.org/10.1007/s00382-009-0551-6>
- Zanin PR, Satyamurty P (2020) Hydrological processes interconnecting the two largest watersheds of South America from multi-decadal to inter-annual time scales: a critical review. *Int J Climatol* 40(9):4006–4038
- Zemp DC, Schleussner CF, Barbosa HM, Hirota M, Montade V, Sampaio G, Staal A, Wang-Erlandsson L, Rammig A (2017) Self-amplified amazon forest loss due to vegetation-atmosphere feedbacks. *Nat Commun* 8:14681. <https://doi.org/10.1038/ncomms14681>
- Zeng X, Zhao M, Dickinson RE (1998) Intercomparison of bulk aerodynamic algorithms for the computation of sea surface fluxes using TOGA COARE and TAO data. *J Clim* 11(10):2628–2644
- Zhang X, Liu H, Zhang M (2015) Double ITCZ in coupled Ocean-Atmosphere models: from CMIP3 to CMIP5. *Geophys Res Lett* 42(20):8651–8659. <https://doi.org/10.1002/2015GL065973>